We are IntechOpen,
the world's leading publisher of
Open Access books
Built by scientists, for scientists

5,500
Open access books available

136,000
International authors and editors

170M
Downloads

154
Countries delivered to

Our authors are among the

TOP 1%
most cited scientists

12.2%
Contributors from top 500 universities

BOOK CITATION INDEX
CLARIVATE ANALYTICS
INDEXED

WEB OF SCIENCE™

Selection of our books indexed in the Book Citation Index
in Web of Science™ Core Collection (BKCI)

Interested in publishing with us?
Contact book.department@intechopen.com

Chapter

Non-equilibrium Equation of State in the Approximation of the Local Density Functional and Its Application to the Emission of High-Energy Particles in Collisions of Heavy Ions

A.T. D'yachenko and I.A. Mitropolsky

Abstract

The non-equilibrium equation of state is found in the approximation of the functional on the local density, and its application to the description of the emission of protons and pions in heavy ion collisions is considered. The non-equilibrium equation of state is studied in the context of the hydrodynamic approach. The compression stage, the expansion stage, and the freeze-out stage of the hot spot formed during the collisions of heavy ions are considered. The energy spectra of protons and subthreshold pions produced in collisions of heavy ions are calculated with inclusion of the nuclear viscosity effects and compared with experimental data for various combinations of colliding nuclei with energies of several tens of MeV per nucleon.

Keywords: local density functional, hydrodynamics, non-equilibrium equation of state, heavy ions, hot spot, nuclear viscosity, protons, subthreshold pions

1. Introduction

The main object of studying heavy ion collisions is to study the equation of state (EOS) of nuclear matter. Along with molecular dynamics and the Vlasov dynamic equation, nuclear hydrodynamics is an effective method for describing the interaction of heavy ions with medium and intermediate energies (see, e.g., [1]). Typically, the equilibrium EOS is used [1]; it involves the local thermodynamic equilibrium in the system. A hybrid model was proposed for use at high energies in [2, 3]. It includes a fast non-equilibrium stage and the subsequent description of the dynamics of a nucleus-nucleus collision based on equilibrium relativistic hydrodynamics of an ideal fluid. We showed in our works [4–11] that local thermodynamic equilibrium is not immediately established in the process of collisions of heavy ions, since the non-equilibrium component of the distribution function, which leads to the formation of a collisionless shock wave, is important at the compression stage.

The kinetic equation for finding the distribution function of nucleons is used in this paper. It is solved in conjunction with the equations of hydrodynamics, which are essentially local conservation laws of mass, momentum, and energy. As a result, the non-equilibrium equation of state is found in the approximation of the functional on the local density. Since the emitted secondary particles (nucleons, fragments, and pions) contain the basic information about the EOS, it is necessary to know the differential cross sections for the emission of these particles. The energy spectra of protons and subthreshold pions with allowance for nuclear viscosity are analyzed in this paper as a follow-up to our works [11–13] devoted to the energy spectra of protons and fragments in which viscosity was neglected.

By subthreshold production, we mean the generation of π mesons with energies lower than the threshold for the production of pions E_{NN} in free nucleon-nucleon collisions. The absolute thresholds for pion production are $E_{NN} = 2m_\pi + \frac{m_\pi^2}{2m} \approx 290$ MeV in nucleon-nucleon collisions, $E_{NA} \approx m_\pi \approx 140$ MeV in nucleon-nucleus collisions, and $E_{BA} = \frac{m_\pi^2 + 2(A+B)m_\pi m}{2ABm} \approx 20$ MeV in nucleus-nucleus collisions at $A = B = 12$, where m_π is the pion mass and m is the nucleon mass. This expression for the absolute threshold energy is obtained from a comparison of the relativistic invariants $J = E^2 - P^2$ before and after the collision, neglecting the binding energy of pion (E is the total energy; P is the total momentum).

The pion production threshold during the collision of heavy ions decreases owing to collective effects and the internal motion of nucleons. These effects are naturally taken into account using the hydrodynamic approach, which explicitly includes the many-particle nature of colliding heavy ions. In the case of low energies, the hydrodynamics should be modified to take into account the non-equilibrium EOS, which describes the transition from the initial non-equilibrium state to the state of local thermodynamic equilibrium.

Such an approach to describing the temporal evolution of the resulting hot spot includes a compression stage and an expansion stage taking into account the nuclear viscosity that we found. The calculated energy spectra of protons and pions produced in nuclear collisions (both identical and different in mass) at an energy of 92 MeV per nucleon in the case of protons and 94 MeV per nucleon in the case of subthreshold pions are in agreement with the available experimental data [1, 14], respectively.

2. Non-equilibrium equation of state in a local density approximation

If the energies of colliding heavy ions are less than 300 MeV per nucleon (pion production threshold in free nucleon-nucleon collisions), we use the kinetic equation to find the nucleon distribution function $f\left(\vec{r}, \vec{p}, t\right)$ ($\vec{r}(x_1, x_2, x_3)$ is the spatial coordinate; $\vec{p}(p_1, p_2, p_3)$ is the momentum; t is the time) [11, 12]:

$$\frac{\partial f}{\partial t} + \frac{p_i}{m} \frac{\partial f}{\partial x_i} - \frac{\partial W}{\partial x_i} \frac{\partial f}{\partial p_i} = \frac{f_0 - f}{\tau}, \tag{1}$$

where $f_0\left(\vec{r}, \vec{p}, t\right)$ is a local equilibrium distribution function; τ is the relaxation time; $W(\rho)$ ($W(\rho) = \alpha\rho + \beta\rho^\gamma$) is a one-particle Skyrme-type self-consistent potential depending on the density ρ, where three parameters $\alpha(\alpha < 0)$, $\beta(\beta > 0)$, and $\gamma(\gamma > 1)$ are determined by setting the equilibrium density $\rho_0 = 0.145$ fm^{-3}, binding energy $E_b = -16$ MeV, and compression modulus $K = 210$ MeV; and m is the nucleon mass.

Equation (1) with allowance for the hydrodynamic equations obtained from (1) by taking the corresponding moments with a weight of 1, $\vec{p}$, and $\frac{p^2}{2m}$ [11, 12] describes the dynamics of nuclear collisions and forms the basis of our approach. The solution of Eq. (1) can be simplified if we work out the distribution function $f\left(\vec{r},\vec{p},t\right)$ determining EOS in the form

$$f\left(\vec{r},\vec{p},t\right) = f_1 q + f_0(1-q),\tag{2}$$

where the distribution function $f_1\left(\vec{r},\vec{p},t\right)$ is defined in momentum space as an axially symmetric Fermi ellipsoid, which is a convenient form for describing excitations in the Fermi liquid theory and is assumed to be blurred along the axis p_1 with the temperature T_1 and frozen in the transverse directions p_2 and p_3. The function $f_0\left(\vec{r},\vec{p},t\right)$ is represented in the momentum space by the equilibrium Fermi sphere blurred with temperature T; q is a relaxation factor ($q = \exp\left(-\int_{t_0}^{t} dt/\tau\right)$), where $t_0\left(\vec{r},t\right)$ is the start time of the relaxation process in the system; τ is the relaxation time, which can be specified as in [15]. However, we define τ more traditionally as $\tau = \lambda/v_T$, where λ is the mean free path of nucleons at a given nucleon density, which is assumed to be equal to the mean distance between nucleons, and v_T is the mean speed of the thermal Fermi motion of nucleons. This expression for τ in the energy range under consideration is close in magnitude to the value proposed in [15], but it turns out to depend on temperature and compression ratio and seems to us more realistic. All calculations are carried out precisely for such τ. The equation for finding the relaxation factor $q\left(\vec{r},t\right)$ is obtained by taking the moment for the kinetic equation with a weight of $p_1^2 - (p_2^2 + p_3^2)/2$ that determines the degree of anisotropy of the distribution function $f\left(\vec{r},\vec{p},t\right)$ in momentum space.

So, the initial moments $\int \frac{d^3\vec{p}}{(2\pi\hbar)^3}$ with weights 1, $\vec{p}$, $\frac{p^2}{2m}$, $p_1^2 - (p_2^2 + p_3^2)/2$ from kinetic equation (1) provide the corresponding hydrodynamic equations [11, 12] for finding nucleon density $\rho\left(\vec{r},t\right)$, velocity field $\vec{v}\left(\vec{r},t\right)$, internal energy density $e = \varepsilon + I + e_{int}$, and pressure tensor $P_{ij} = P_{(kin)ij} + P_{int}\delta_{ij}$ (the repeated indices imply the summation, δ_{ij} is the Kronecker symbol). The terms of interaction for energy density e_{int} and pressure P_{int} are, respectively,

$$e_{int} = \int_0^\rho W(\rho)d\rho, \quad P_{int} = \rho^2 \frac{d(e_{int}/\rho)}{d\rho}.$$

The kinetic terms are.

$\varepsilon = \frac{3}{10}\frac{\hbar^2}{m}\left(\frac{3}{2}\pi^2\rho\right)^{2/3}\rho$, $\varepsilon_1 = \frac{\hbar^2}{10m}\left(\frac{3}{2}\pi^2\rho_0\right)^{2/3}\frac{\rho^3}{\rho_0^2}$, $\varepsilon_2 = \frac{\hbar^2}{10m}\left(\frac{3}{2}\pi^2\rho_0\right)^{2/3}\rho$,

$P_{kin}^{||} = P_{(kin)11} = 2(\varepsilon_1 + I_1)q + \frac{2}{3}(\varepsilon + I)(1-q)$,

$P_{kin}^{\perp} = P_{(kin)22} = P_{(kin)33} = 2\varepsilon_2 q + \frac{2}{3}(\varepsilon + I)(1-q)$,

which corresponds to diagonal tensor of pressure $P_{(kin)ij} = 0 (i \neq j)$, and heat terms I and I_1 are associated with temperatures T and T_1, respectively. Since we assume that the integrals of motion (density ρ, momentum density $m\rho\vec{v}$, and

energy density ($\varepsilon + I = \varepsilon_1 + 2\varepsilon_2 + I_1$)) are conserved during relaxation, hydrodynamic equations have no right-hand sides.

To find density ρ, velocity field $\vec{\upsilon}$ relaxation factor q, and temperatures T and T_1, we thus have the closed system of equations that considers expressions for terms of interaction and kinetic terms. These equations allow us to find distribution function $f\left(\vec{r}, \vec{p}, t\right)$ in form (2). Relaxation factor $q(0 \leq q \leq 1)$ allows us to describe the dynamics of the Fermi surface variation from the state with $q = 1$, where function $f\left(\vec{r}, \vec{p}, t\right)$ in the momentum space is maximally anisotropic, to the state with $q = 0$, where it is completely isotropic.

3. Hydrodynamic stage

We simplify the description of the time evolution of colliding nuclei distinguishing the compression stage, the expansion stage, and the freeze-out stage of the resulting hot spot. We reduce the interaction between two nuclei to the interaction between their overlapping regions. This can be interpreted as a hot spot formation process. In this case, we take into account the conservation laws. Shock waves with changing front diverging in opposite directions are formed at the stage of compression during the interaction between overlapping regions of colliding nuclei [5–9].

In the process of compression, when the shock wave reaches the boundaries of the hot spot, the density reaches its maximum value. The dependence of the maximum compression ratio ρ/ρ_0 at the shockwave front (solid line) on the collision energy of nuclei E_0 is shown in **Figure 1**. It hardly depends on the composition of colliding nuclei, since we consider the interaction of the same overlapping regions in the system of equal speeds of the colliding nuclei. The dependence of ρ/ρ_0 on the energy E_0 for the distribution function corresponding to the equilibrium EOS with $q = 0$ is shown by a dashed line, and such a dependence for a completely non-equilibrium EOS with $q = 1$ is shown by a dash-dotted line.

The relaxation factor at the energy region of $E_0 < 100$ MeV per nucleon is maximal ($q = 1$), and it decreases with increasing energy, leading to a greater isotropy of the distribution function. We calculated the dependence of the maximum compression ratio on energy for $E_0 > 100$ MeV per nucleon. It is found in between the extreme cases with $q = 0$ and $q = 1$. At $E_0 < 100$ MeV per nucleon, the dependence ρ/ρ_0 on energy coincides with the dash-dotted curve corresponding to the case with $q = 1$ (i.e., completely non-equilibrium EOS) and is located above the dashed curve corresponding to the case with $q = 0$ belonging to traditional hydrodynamics and the onset of local thermodynamic equilibrium.

A compressed and heated hot spot (a ball with radius R) expands when the shock wave reaches the boundaries of the system. The hot spot expands in accordance with the equations of hydrodynamics for radial motion of nucleon density $\rho(r, t)$, velocity $\upsilon(r, t)$, energy density $e(r, t)$, and pressure $P(r, t)$, following from (1) [11, 12]:

$$\frac{\partial \rho}{\partial t} + \frac{\partial (r^2 \rho \upsilon)}{r^2 \partial r} = 0, \tag{3}$$

$$\frac{\partial (m \rho \upsilon)}{\partial t} + \frac{\partial (r^2 m \rho \upsilon^2)}{r^2 \partial r} + \frac{\partial P}{\partial r} = 0, \tag{4}$$
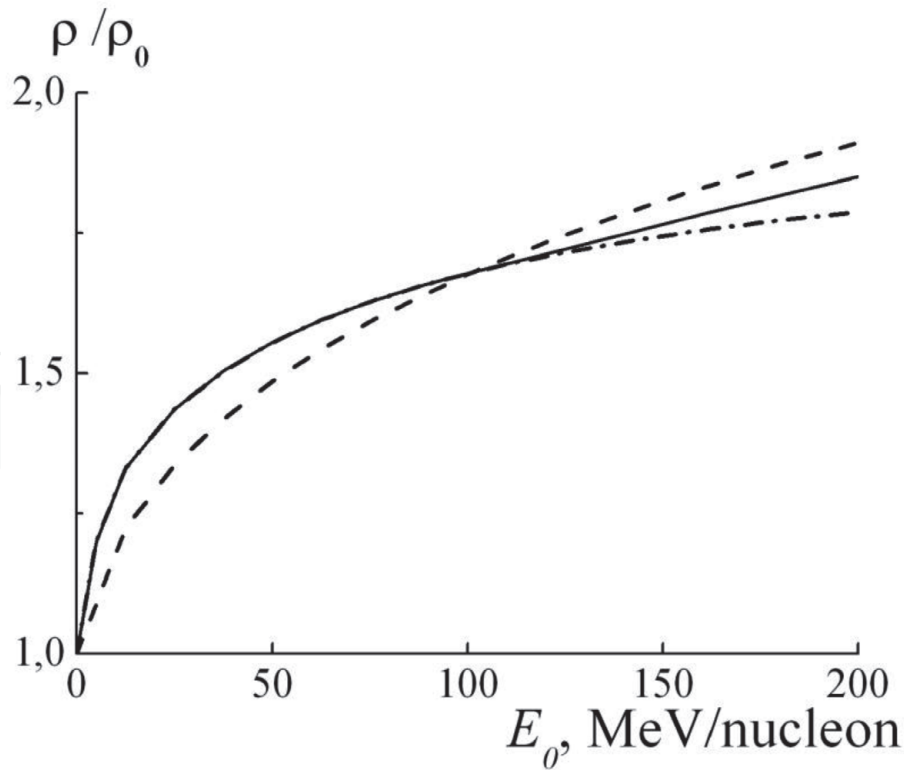
Figure 1.
The dependence of the maximum compression ratio ρ/ρ_0 on the collision energy E_0 achieved during the interaction of the overlapping regions of colliding nuclei for the case of the relaxation factor q calculated by us (solid line), for the case where the factor $q = 0$ (dashed line) and for the case where $q = 1$ (dash-dotted line). All dependences correspond to the value of the compression modulus $K = 210$ MeV.

$$\frac{\partial(m\rho v^2/2 + e)}{\partial t} + \frac{\partial(r^2 v(m\rho v^2/2 + e + P))}{r^2 \partial r} = 0. \tag{5}$$

The heat flux for a local equilibrium distribution function is $Q = 0$. Here, the internal energy density is $e = e_{kin} + e_{int}$ and pressure is $P = P_{kin} + P_{int}$, where e_{kin} and P_{kin} are the kinetic terms, and the interaction terms e_{int} and P_{int} are.

$$e_{int} = \int_0^\rho W(\rho)d\rho, \; P_{int} = \rho^2 \frac{d(e_{int}/\rho)}{d\rho}. \tag{6}$$

The velocity field is found from Eq. (3) in the approximation of a homogeneous but time-dependent density of hot spot $\rho(r,t) = \rho(t)$:

$$v(r,t) = \frac{\dot{R_1}}{R_1}r, \; 0 \le r \le R_1, \tag{7}$$

$$v(r,t) = \frac{\dot{R}(r - R_1) - \dot{R_1}(r - R)}{(R - R_1)}, \; R_1 \le r \le R, \tag{8}$$

where $R(t)$ is the radius of the hot spot; $R_1(t)$ is the radius of the velocity field kink determined from the solution of equations; and $\dot{R}(t)$ and $\dot{R_1}(t)$ are the derivatives in time (speed), which are also found from the Eqs. A system of ordinary integro-differential equations is obtained after integrating Eqs. (4) and (5) over the hotspot volume. It is solved numerically.

However, the deviation of the distribution function $f\left(\vec{r},\vec{p},t\right)$ from the local equilibrium function $f_0\left(\vec{r},\vec{p},t\right)$ is not taken into account in these equations. Expressing $f\left(\vec{r},\vec{p},t\right)$ from the right side of Eq. (1) through its left side, we find

$$f = f_0 - \tau\left(3 - \frac{5}{3}I\frac{\partial}{\partial I}\right)f_0\frac{\partial v}{\partial r}, \tag{9}$$

where I is the thermal term depending on the temperature T. When obtaining (9), we substituted $f_0\left(\rho(r,t),U\left(r,\vec{p},t\right),T(r,t)\right)$ into the left part of Eq. (1) instead of $f\left(r,\vec{p},t\right)$, taking into account Eqs. (3)–(5), where $U = \frac{(\vec{p}-m\vec{v})^2}{2m}$. In this case, the hot spot was averaged over the volume to derive Eq. (1), and at the expansion stage, the density $\rho(r,t)$, the temperature $T(r,t)$, and the thermal term $I(r,t)$ were considered to be homogeneous functions of time t and independent of the radius r. Substituting expression (9) into the equations of hydrodynamics [11, 12], we find the corrections to kinetic terms of the energy density e_{kin} and pressure P_{kin}:

$$e_{kin} = e_{0,kin} - \tau\frac{4}{3}\left(e_{0,kin} + \frac{5}{4}e_F\right)\frac{\partial v}{\partial r} = e_{0,kin} - \frac{3}{2}\eta\frac{\partial v}{\partial r}, \tag{10}$$

$$P_{kin} = P_{0,kin} - \tau\frac{4}{3}\left(P_{0,kin} + \frac{5}{6}e_F\right)\frac{\partial v}{\partial r} = P_{0,kin} - \eta\frac{\partial v}{\partial r}. \tag{11}$$

where $e_{0,kin} = e_F + I$ and $P_{0,kin} = \frac{2}{3}e_{0,kin}$ are the equilibrium kinetic parts of the energy density and pressure density, $e_F = \frac{3}{10}\frac{\hbar^2}{m}\left(\frac{3}{2}\pi^2\rho\right)^{2/3}\rho$, and $\eta = \frac{4}{3}\left(P_{0,kin} + \frac{5}{6}e_F\right)\tau$ is the viscosity coefficient. The following correction terms turn out to be an order of magnitude smaller and they are not taken into account. The heat flux is $Q = 0$. The corrections to kinetic terms significantly affect the hotspot expansion and slow it down, because the Reynolds number is not large $Re = \frac{m\rho vl}{\eta} \sim 1$ for the viscosity coefficient η found by us (formula (10)) in the energy range under consideration of $E_0 \approx 100$ MeV per nucleon with a characteristic nuclear size of $l \approx 3$ fm. In our case, the temperature is $T \approx 20$ MeV; $P_{0,kin} \approx \rho T$; $\tau \approx 3\cdot10^{-23}$ s; the viscosity coefficient is $\eta \approx 4\cdot10^{10}$ kg m^{-1} s^{-1}. It coincides in the order of magnitude with the gas estimate $\eta \sim \sqrt{mT}/\sigma$ [16] if we take $\sigma \approx 40$ mb for the elementary cross section. Moreover, $\eta s >> \frac{\hbar}{4\pi}$, where s is the entropy density ($s \sim \rho$). That is, in our case, the ratio $\frac{\eta}{s}$ is more than an order of magnitude higher than the limiting value of $\frac{\hbar}{4\pi}$ [17] (achievable, e.g., in the state of a quark-gluon plasma). Thus, the viscosity coefficient is quite large in the energy range under consideration. This reduces the expansion speed of the hot spot and increases its temperature. Secondary particles (nucleons, fragments, and pions) form and freeze out when the expanding nuclear system reaches a critical density (freezing density) ρ^* determined from the condition $\frac{dP_{int}}{d\rho} = \rho\frac{dW}{d\rho} = 0$.

4. Double differential cross sections of the emission of protons and pions: comparison with the experimental data

Protons and pions are emitted when the nuclear system reaches a critical density. The cross section of the emission of protons (pions) is found from the condition that the number of particles $fd^3\vec{p}$ and the value $d^3\vec{p}/E$ of are relativistic

invariants [18, 19]. As a result, the inclusive double differential cross section of reaction A + B → p(π) + X is

$$\frac{d^2\sigma}{dEd\Omega} = (2S+1)\frac{2\pi}{(2\pi\hbar)^3}\int G(b)bdb\int d\vec{r}\,\gamma\left(E - \vec{p}\vec{v}\right)pf\left(\vec{r},\vec{p},t\right), \qquad (12)$$

where *b* is an impact parameter and the distribution function of protons (pions) has the form

$$f\left(\vec{r},\vec{p},t\right) = \left[\exp\left(\frac{\gamma\left(E - \vec{p}\vec{v} - \mu\right)}{T}\right) \pm 1\right]^{-1}. \qquad (13)$$

Here E and $\vec{p}$ are the total energy and momentum of the proton (pion), respectively; $E = \sqrt{p^2 + m_{p(\pi)}^2}$; Ω is the solid angle; S is the spin; $\vec{v}\left(\vec{r},t\right)$ and $T\left(\vec{r},t\right)$ are the velocity field and temperature at the time of freeze-out (they are solutions of the equations of hydrodynamics); $\gamma = 1/\sqrt{1 - (v/c)^2}$ is the Lorentz factor; μ is the chemical potential (for pions $\mu = 0$, because the number of pions is not specified). The factor $G(b) = \sigma_t(b)/\sigma_g(b)$ introduced in (12) takes into account the difference between the total cross section and the geometric cross section, where $\sigma_t(b)$ is defined as the cross section of the formation of a hot spot for a given impact parameter *b* from two overlapping regions in colliding nuclei, and $\sigma_g(b)$ is equal to the geometric cross section of these overlapping regions. Here, the total cross section is always greater than geometric one, as in the case of the fusion of two nuclei comparable in size. In addition, the function $f\left(\vec{r},\vec{p},t\right)$ included in Eq. (12) was modified in comparison with Eq. (13) according to relation (2): the sign "+" refers to protons, and the sign "−" refers to pions. Expressions (12) and (13) refer to protons (pions) emitted from a hot spot as a result of the interaction of the overlapping regions of colliding nuclei. In addition to this contribution, we took into account the contribution from the emission of protons (pions) as a result of the fusion of non-overlapping regions of colliding nuclei. The calculated double differential cross sections of proton emission (energy spectra) were compared with similar calculations obtained by solving the Vlasov-Uling-Uhlenbeck (VUU) kinetic equation [1] and with available experimental data. Our calculations corresponded to the equation of state with selected compression modulus equal to $K = 210$ MeV, i.e., with the same which was taken for the best description of the experiment in the calculations that we performed in [8, 9] at energies of 250 and 400 MeV per nucleon for colliding Ne and U nuclei.

We present the proton spectra in the ^{40}Ar + ^{40}Ca → p + X reaction at the angles of 30° (*1*), 50° (*2*), 70° (*3*), and 90° (*4*) for the energy of projectile nuclei of ^{40}Ar of 92 MeV per nucleon (**Figure 2**). In **Figure 2**, the solid curves correspond to our calculation, the histograms correspond to the calculations performed by the method of solving the VUU equation [1], and the dots are the experimental data from [1].

As can be seen, our calculation (this is not the Monte Carlo method and not histograms) is in good agreement with the experimental data. This is especially true for small angles of emission of protons (30°, 50°, and 70°). Our approach has an advantage over the more detailed method of solving the VUU equation [1], since the solid curves (but not histograms) are the result of the calculation. Note here that simple cascade models, as mentioned in [1], cannot describe these experimental data at all.
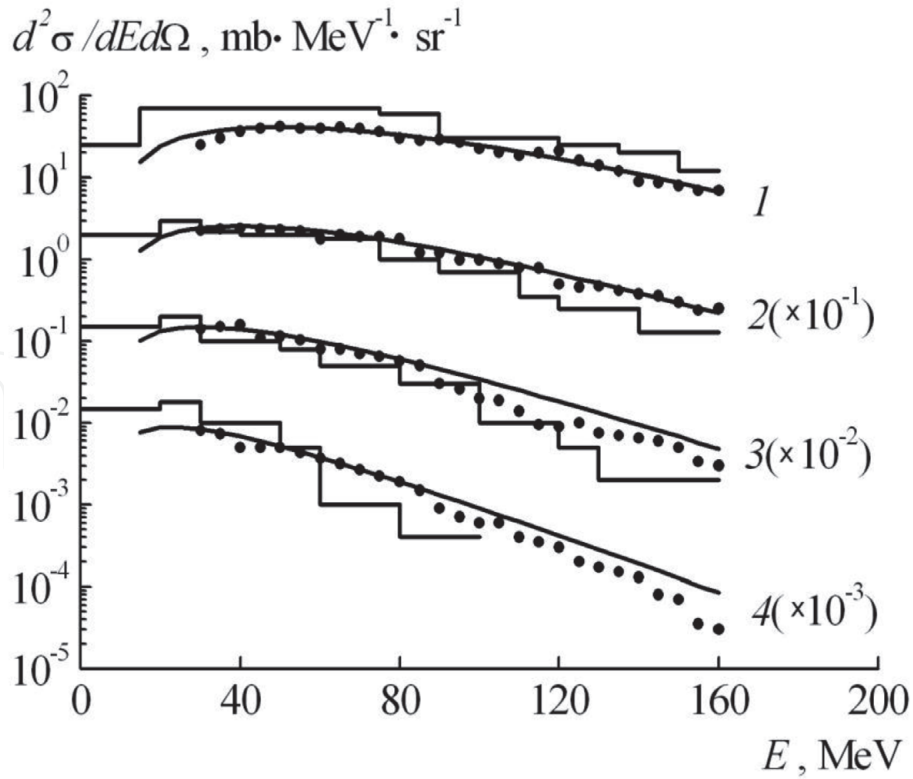
Figure 2.
Spectra of protons emitted in the reaction $^{40}Ar + {}^{40}Ca$ with the energy of ^{40}Ar ions of 92 MeV per nucleon at angles of 30° (1), 50° (2), 70° (3), and 90° (4). The solid lines are the results of calculations according to this model with the calculated q corresponding to K = 210 MeV; the histograms are the results of calculations obtained from the solution of the VUU kinetic equation (1); the dots are the experimental data from [1].
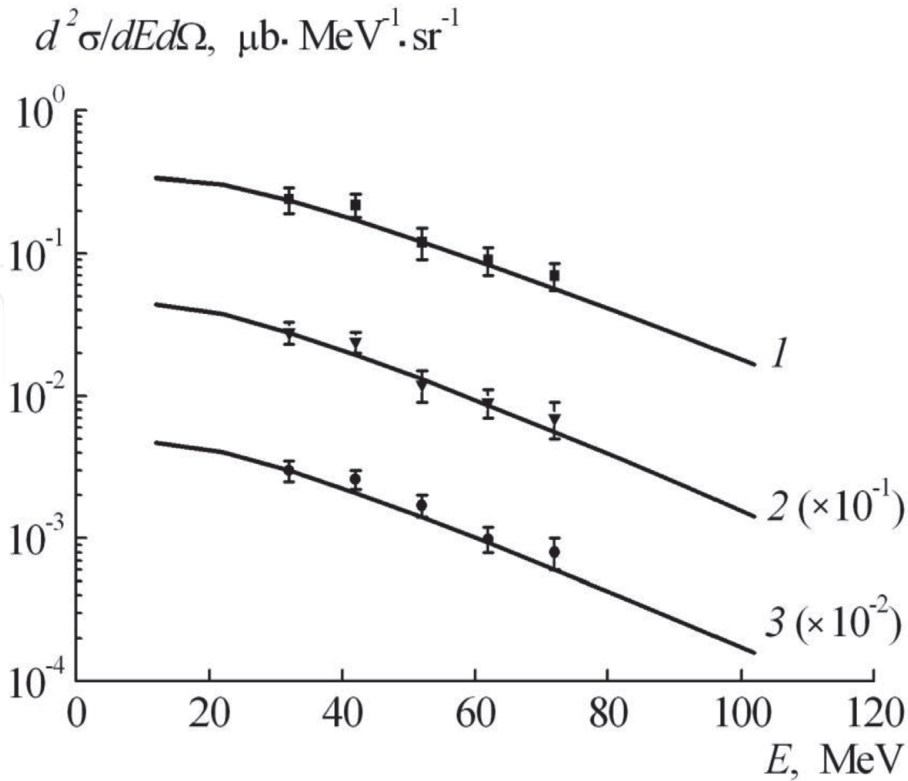
Figure 3.
The calculated (solid lines) and experimental (dots) [14] inclusive double differential cross sections of the emission of mesons at the observation angle of 90° in the reactions $^{16}O + {}^{27}Al$ (1), $^{16}O + {}^{58}Ni$ (2), and $^{16}O + {}^{197}Au$ (3) with energy of ^{16}O ions of $E_0 = 94$ MeV per nucleon.
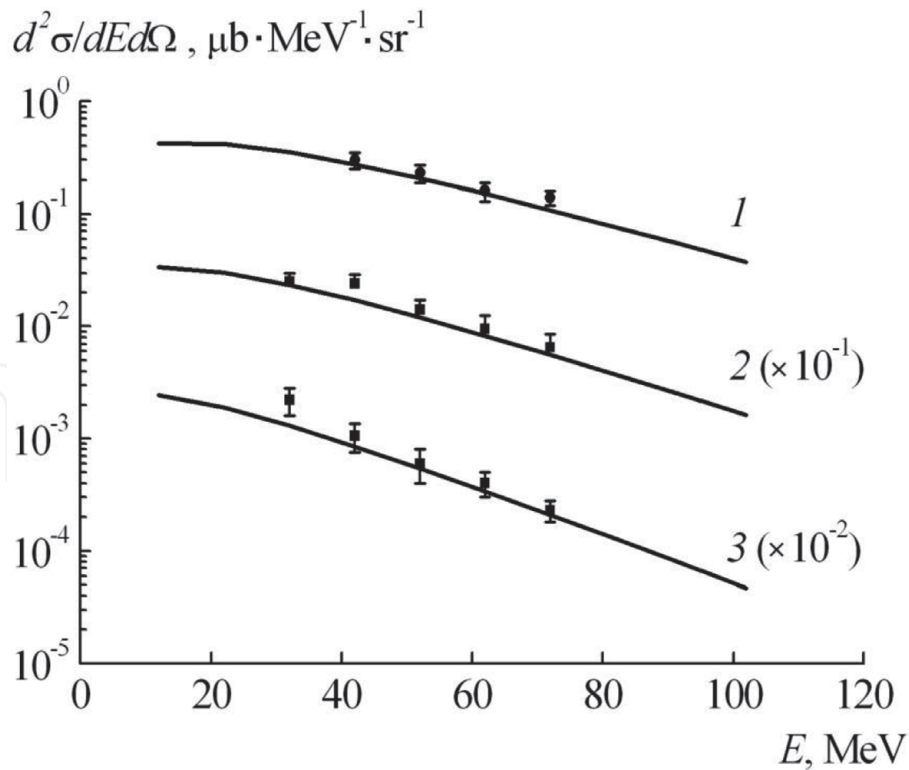
Figure 4.
The calculated (solid curves) and experimental (dots) [14] inclusive double differential cross sections of the emission of mesons in the reaction ^{16}O + ^{27}Al with energy of ^{16}O ions of 94 MeV per nucleon at the observation angles of 70° (curve 1), 90° (curve 2), and 120° (curve 3).

We compared our data with the available experimental data on the emission of pions. **Figure 3** illustrates the comparison of our calculated (solid lines) and experimental [14] (dots) double differential cross sections for the reactions of π^+-meson production when ^{16}O ions collide with ^{27}Al nuclei (curve *1*), ^{58}Ni nuclei (curve *2*), and ^{197}Au nuclei (curve *3*) at energies of ^{16}O ions of $E_0 = 94$ MeV per nucleon at an angle of 90°. It can be seen that the calculation is in good agreement with the experiment for chosen parameters of the nuclear interaction and taking into account the viscosity of the medium η that is found by us and proportional to the relaxation time τ within the experimental errors. In this case, the effect of viscosity on the calculated cross section of emitted pions is stronger for more asymmetric combinations of colliding nuclei, when the contribution of the emission of pions from the hot spot prevails. Thus, inclusive pion spectra in asymmetric nuclear collisions can be used to measure the viscosity of a nuclear medium.

Figure 4 illustrates the comparison of the calculations (solid lines) with the experimental data [14] (dots) for the reaction ^{16}O + $^{27}Al \rightarrow \pi^+ + X$ at energy of ^{16}O ions of 94 MeV per nucleon at pion emission angles of 70° (curve *1*), 90° (curve *2*), and 120° (curve *3*). The calculation is in agreement with the experimental data if its parameters are constant. In all the illustrations under consideration, the agreement of calculation with the experiment was achieved without introducing fitting parameters and is more successful than our previous works [11, 19, 20].

5. Conclusions

Thus, the idea of using the hydrodynamic approach with a non-equilibrium equation of state in describing collisions of heavy ions is further developed in this work. The non-equilibrium equation of state is found in the approximation of the

functional on the local density. The differential cross sections of the emission of protons and the production of subthreshold pions in heavy ion collisions are uniformly described with the same fixed parameters of the equation of state and in the same approach as in the previous papers [11–13], which describe the differential cross sections for the formation of protons and light fragments. It is shown that the non-equilibrium equation of state included in the hydrodynamic equations allows us to describe the experimental energy spectra of protons produced in collisions of heavy ions with intermediate energies better than the equation of state corresponding to traditional hydrodynamics, which initially implies the local thermodynamic equilibrium.

This simplified hydrodynamic approach including a description of the stages of compression, expansion, and freeze-out of a substance during heavy ion collisions turned out to be no worse than a more detailed approach based on the Monte Carlo solution of the Vlasov-Uling-Uhlenbeck kinetic equation.

In comparison with previous works, the inclusion of the effects of nuclear viscosity, which we found in the relaxation approximation for the kinetic equation, is new. This did not add new parameters in describing the temporal evolution of nuclear collisions. The relaxation time τ, which determines the nuclear viscosity coefficient η, turned out to be close to the value found on the basis of the behavior of nuclear Fermi liquid [15] and is not a fitting parameter. When describing the emission of protons and fragments, the inclusion of the viscosity of the medium is not so significant, and the pions are very sensitive to the viscosity.

The highlighting of proton (pion) emission after the temporal evolution of the resulting hot spot and the contribution to the particle emission cross sections during the fusion of "spectators" (non-overlapping regions of colliding nuclei) were significant in calculating the cross sections. This made it possible to describe the differential cross sections of the emission of protons (pions) for collisions of nuclei in various combinations. Highlighting this feature of our approach can be useful in comparison with other ways of pion production in heavy ion collisions, for example [21, 22], based on the solution of the Vlasov-Uling-Uhlenbek equation. These works include a range of higher energies of colliding heavy ions (more than 300 MeV per nucleon) and the production of pions by means of Δ-isobar production. We included this channel at low subthreshold energies, not limited to the production of thermal pions. However, this channel appears on the higher energy tails of the energy spectra of pions [23].

Studies of the formation of protons, fragments, and subthreshold production of pions may be of interest for the development of a scientific program planned with radioactive beams in Dubna using the COMBAS facility [24], which is designed to study nuclear collisions in the energy range of 20–100 MeV per nucleon.

Author details

A.T. D'yachenko[1*] and I.A. Mitropolsky[2]

1 Emperor Alexander I St. Petersburg State Transport University, St. Petersburg, Russia

2 Petersburg Nuclear Physics Institute, National Research Center Kurchatov Institute, Gatchina, Russia

*Address all correspondence to: dyachenko_a@mail.ru

IntechOpen

References

[1] Stocker H, Greiner W. High energy heavy ion collisions—probing the equation of state of highly excited hardronic matter. Physics Reports [Internet]. Elsevier BV; May 1986;**137** (5-6):277-392. DOI: 10.1016/0370-1573 (86)90131-6

[2] Khvorostukhin AS, Toneev VD. Hadron rapidity spectra within a hybrid model. Physics of Particles and Nuclei Letters [Internet]. Pleiades Publishing Ltd; January 2017;**14**(1):9-17. DOI: 10.1134/s1547477117010162

[3] Khvorostukhin AS, Toneev VD. Rapidity distributions of hadrons in the HydHSD hybrid model. Physics of Atomic Nuclei [Internet]. Pleiades Publishing Ltd; March 2017;**80**(2):285-298. DOI: 10.1134/s1063778817010112

[4] D'yachenko AT. Physics of Atomic Nuclei. 1994;**57**:1930

[5] D'yachenko AT, Gridnev KA. Calculation scheme of heavy-ion collisions within the framework of a modified hydrodinamic approach. Bulletin of the Russian Academy of Sciences: Physics [Internet]. Allerton Press; July 2013;**77**(7):857-861. DOI: 10.3103/s1062873813070095

[6] D'yachenko AT, Gridnev KA, Greiner W. Calculation of heavy ion collisions within the framework of the modified hydrodynamic approach. Journal of Physics G: Nuclear and Particle Physics [Internet]. IOP Publishing; 20 June 2013;**40**(8): 085101. DOI: 10.1088/0954-3899/40/8/085101

[7] D'yachenko AT, Gridnev KA. Calculation of heavy-ion collisions within the framework of the hydrodynamic approach with a nonequilibrium equation of state. Bulletin of the Russian Academy of Sciences: Physics [Internet]. Allerton

Press; July 2014;**78**(7):648-653. DOI: 10.3103/s1062873814070107

[8] D'yachenko AT, Gridnev KA, Mitropolsky IA. Features of a nonequilibrium equation of state in heavy-ion collisions at intermediate energies. Bulletin of the Russian Academy of Sciences: Physics [Internet]. Allerton Press; July 2015;**79**(7):858-863. DOI: 10.3103/s1062873815070096

[9] AT D'yachenko, K. A. Gridnev, I. A. Mitropolsky, and W. Greiner. In: YE Penionzhkevich and YG Sobolev editors. Proceedings of the 7th International Symposium on Exotic Nuclei, Kaliningrad, Russia, 2014, World Scientific, Singapore; 2015. p. 413

[10] D'yachenko AT, Mitropolsky IA. Vopr. At Nauki Tekh., Ser.: Yad.-Reakt. Konst. 2016;**2**:94

[11] D'yachenko AT, Mitropolsky IA. A nonequilibrium equation of state in heavy-ion collisions at intermediate energies. Bulletin of the Russian Academy of Sciences: Physics [Internet]. Allerton Press; August 2016; **80**(8):916-920. DOI: 10.3103/ s1062873816080104

[12] D'yachenko AT, Mitropolsky IA. Fragments in heavy ion collisions in a hydrodynamic approach with a nonequilibrium equation of state. Bulletin of the Russian Academy of Sciences: Physics [Internet]. Allerton Press; December 2017;**81**(12):1521-1526. DOI: 10.3103/s1062873817100112

[13] D'yachenko AT, Mitropolsky IA, Sobolev YG. In: Penionzhkevich YE, Sobolev YG, editors. Proceedings of the 8th International Symposium on Exotic Nuclei, Kazan, Russia, 2016, World Scientific, Singapore; 2017. p. 38

[14] Badala A, Barbera R, Bonasera A, Di Toro M, Palmeri A, Pappalardo GS, et al.

Statistical and microscopic description of energetic products in the reactions induced by O16 on Al27, Ni58, and Au197 at 94 MeV/nucleon. Physical Review C [Internet]. American Physical Society (APS); 1 January 1991;**43**(1): 190-200. DOI: 10.1103/physrevc.43.190

[15] Bertsch G. The collision integral in nuclear matter at zero temperature. Zeitschrift für Physik A. Atoms and Nuclei [Internet]. Springer Science and Business Media LLC; March 1978;**289** (1):103-115. DOI: 10.1007/bf01408501

[16] Lifshitz EM, Pitaevskii LP. Course of Theoretical Physics. In: Physical Kinetics. Vol. 10. (Pergamon, Oxford, 1981; Nauka, Moscow, 1979). [Publishing: 1 January 1981]

[17] Kovtun PK, Son DT, Starinets AO. Viscosity in strongly interacting quantum field theories from black hole physics. Physical Review Letters [Internet]. American Physical Society (APS); 22 March 2005;**94**(11). DOI: 10.1103/physrevlett.94.111601

[18] Das Gupta S, Mekjian AZ. The thermodynamic model for relativistic heavy ion collisions. Physics Reports [Internet]. Elsevier BV; June 1981;**72**(3): 131-183. DOI: 10.1016/0370-1573(81) 90012-0

[19] D'yachenko AT. Bulletin of the Russian Academy of Sciences: Physics. 1998;**62**:170

[20] D'yachenko AT, Lozhkin OV. Nuclear Physics. 1997;**A696**:81

[21] Zhang Z, Ko CM. Medium effects on pion production in heavy ion collisions. Physical Review C [Internet]. American Physical Society (APS); 7 June 2017;**95** (6). DOI: 10.1103/physrevc.95.064604

[22] Cheng S-J, Yong G-C, Wen D-H. Effects of the symmetry energy in the Sn132+Sn124 reaction at 300 MeV/ nucleon. Physical Review C [Internet].

American Physical Society (APS); 30 December 2016;**94**(6). DOI: 10.1103/ physrevc.94.064621

[23] D'yachenko AT, Baryshnikov VN. On the role of Δ-resonance in the pion production in collisions of heavy intermediate-energy ions in the hydrodynamic approach. Bulletin of the Russian Academy of Sciences: Physics [Internet]. Allerton Press; June 2009;**73** (6):724-726. DOI: 10.3103/ s1062873809060069

[24] Artukh AG, Klygin SA, Kononenko GA, Kyslukha DA, Lukyanov SM, Mikhailova TI, et al. Radioactive nuclear beams of COMBAS facility. Physics of Particles and Nuclei [Internet]. Pleiades Publishing Ltd; January 2016;**47**(1):49-72. DOI: 10.1134/ s1063779616010032